PHILOSOPHICAL TRANSACTIONS A

royalsocietypublishing.org/journal/rsta

Research

Cite this article: Li J, Chen X, Ruschhaupt A. 2022 Fast transport of Bose–Einstein condensates in anharmonic traps. *Phil. Trans. R. Soc. A* **380**: 20210280.
https://doi.org/10.1098/rsta.2021.0280

Received: 11 July 2022
Accepted: 20 September 2022

One contribution of 15 to a theme issue 'Shortcuts to adiabaticity: theoretical, experimental and interdisciplinary perspectives'.

Subject Areas:
quantum physics, atomic and molecular physics, quantum engineering

Keywords:
quantum control, Bose–Einstein condensates, atomic transport, shortcuts to adiabaticity

Author for correspondence:
Jing Li
e-mail: jli@ucc.ie

Fast transport of Bose–Einstein condensates in anharmonic traps

Jing Li[1], Xi Chen[2,3] and Andreas Ruschhaupt[1]

[1]Department of Physics, University College Cork, Cork, T12 H6T1 Ireland
[2]Department of Physical Chemistry, University of the Basque Country UPV/EHU, Apartado 644, 48080 Bilbao, Spain
[3]EHU Quantum Center, University of the Basque Country UPV/EHU, 48940 Leioa, Spain

JL, 0000-0002-7565-3933; XC, 0000-0003-4221-4288; AR, 0000-0002-6044-993X

We present a method to transport Bose–Einstein condensates (BECs) in anharmonic traps and in the presence of atom–atom interactions in short times without residual excitation. Using a combination of a variational approach and inverse engineering methods, we derive a set of Ermakov-like equations that take into account the coupling between the centre of mass motion and the breathing mode. By an appropriate inverse engineering strategy of those equations, we then design the trap trajectory to achieve the desired boundary conditions. Numerical examples for cubic or quartic anharmonicities are provided for fast and high-fidelity transport of BECs. Potential applications are atom interferometry and quantum information processing.

This article is part of the theme issue 'Shortcuts to adiabaticity: theoretical, experimental and interdisciplinary perspectives'.

1. Introduction

The accurate manipulation of ultracold atoms is a key prerequisite to implement quantum technologies within atomic, molecular and optical science [1]. In particular, the transport of individual atoms and of thermal or Bose-condensed clouds using moving traps has been demonstrated in many experiments [2–12] for different goals in quantum information processing and metrology. In all quantum technologies,

THE ROYAL SOCIETY PUBLISHING

preserving quantum coherence and achieving high final fidelities in short times is of crucial importance. One possibility is called shortcuts to adiabaticity (STA) [13,14] which provides a toolbox to control both the internal and external degrees of freedom of a quantum system in faster-than adiabatic times.

Various shortcuts to adiabatic transport have been proposed: Lewis–Riesenfeld invariant-based inverse engineering [15–19], enhanced STA scheme [20–22], the Fourier optimization [23], fast-forward scaling method [24,25] and the counter-diabatic driving [26] have been theoretically put forward, and experimentally demonstrated for various systems [7,10,11,27]. The possibility to operate with short times not only reduces the sensitivity to low-frequency noise, but also allows for improved measurement statistics in the total time available for the experiment.

Different approaches for transporting particles have been implemented. Neutral atoms have been transported as Bose–Einstein condensates (BECs) [2], thermal atomic clouds [28] or individually [5], using magnetic or optical traps. The commonly used traps for ultracold atoms based on electromagnetic fields are never perfectly harmonic. The weak cubic anharmonicity plays a role when a BEC is transported perpendicular to the atom chip surface [29]. The quartic anharmonicity is significant when approximating the potential of an optical tweezers for transport [7,16]. Thus cancelling the anharmonic contributions of the trapping potential is vital for useful control schemes and is already a difficult technical challenge for a static trap [30].

Anharmonicities can have an important impact on the dynamics as observed in atom cooling [31], collective modes [32] or wave packet dynamics [33]. In most cases, the anharmonic traps are considered as a perturbation of a harmonic one. Perturbation theory has been used to design shortcut protocols for expansion/compression [34] and transport [35]. Of course, the results are limited by the premises of perturbation theory, i.e. by small anharmonicities. Considering a non-perturbative scenario is thus of much interest.

In this paper, we propose to inverse engineer rapid and robust transport of an interacting BEC in anharmonic traps using a variational approach. The method relies on a variational formulation of the dynamics to derive a set of coupled Ermakov-like and Newton-like equations, from which the trap trajectory is inferred interpolating between the desired boundary conditions. In §2, we explain the variational formalism. In §3, we work out the explicit solutions for quartic and cubic anharmonicities of the confining potential, and illustrate the efficiency of the method with various numerical examples. In §4, we will discuss the results.

2. Model, Hamiltonian and method

For a cigar-shaped trap with strong transverse confinement, e.g. $\omega_\perp >> \omega$, it is appropriate to consider a one-dimensionless formula by freezing the transverse dynamics to the respective ground state and integrating over the transverse variables [36]. The effective atomic interaction is denoted by $g = 2a_s\omega_\perp N/\omega a_{ho}$, with a_s the interatomic scattering length and $a_{ho} = \sqrt{\hbar/(m\omega)}$. The resulting dimensionless form of Gross–Pitaevskii equation (GPE) [37] can be written as

$$i\frac{\partial\psi(x,t)}{\partial t} = \left[-\frac{1}{2}\frac{\partial^2}{\partial x^2} + V(x,t) + g|\psi(x,t)|^2\right]\psi(x,t), \tag{2.1}$$

where

$$V(x,t) = \frac{1}{2}[x - x_0(t)]^2 + \frac{\kappa}{3!}[x - x_0(t)]^3 + \frac{\lambda}{4!}[x - x_0(t)]^4, \tag{2.2}$$

where $\psi(x,t)$ is the axial wave function of the condensate with normalization condition $\int_{-\infty}^{+\infty}|\psi(x,t)|^2 dx = N$. The attractive and repulsive interactions are denoted by $g < 0$ and $g > 0$, respectively. The axial harmonic trap frequency is ω. The potential centre $x_0(t)$ is time-dependent for transport. Note that the potential in equation (2.2) consists two types of anharmonicities, one is cubic ($\kappa \geq 0$) and the other is quartic ($\lambda \geq 0$) anharmonicity, which is shown in figure 1.

To apply the variational approach, we first define an ansatz for the wave function with a few free parameters and evaluate the Lagrangian density. The minimization of the total Lagrangian

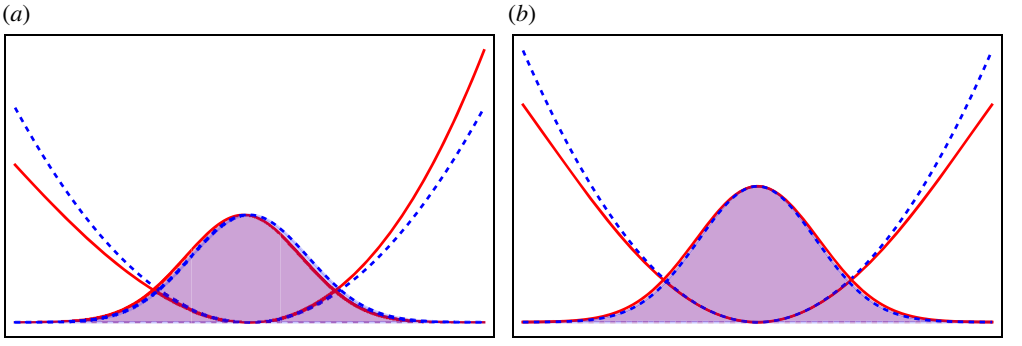

Figure 1. Cubic (*a*) and quartic (*b*) anharmonic potentials (red solid lines) compared with the harmonic counterparts (blue dashed lines). The ground states are plotted for different potentials. (Online version in colour.)

with respect to the free parameters provides equations of motion for the free parameters [38]. This approach is equivalent to a moment method [39].

We assume a general Gaussian ansatz,

$$\psi(x,t) = A(t)\exp\left[-\frac{(x-x_c(t))^2}{2a(t)^2}\right]\exp[ib(t)(x-x_c(t))^2 + ic(t)(x-x_c(t)) + i\phi(t)], \tag{2.3}$$

where the time-dependent parameters $A(t)$, $a(t)$, $b(t)$, $c(t)$ and $\phi(t)$ represent, respectively, the amplitude, width, chirp, velocity and global phase. The wave function centre of mass is $x_c(t)$. In the following, we omit t in those variables for simplification. The normalization condition yields $A = \sqrt{N/(a\sqrt{\pi})}$.

The Lagrangian density which corresponds to equation (2.1) reads [38]

$$L = \frac{i}{2}\left(\frac{\partial\psi}{\partial t}\psi^* - \frac{\partial\psi^*}{\partial t}\psi\right) - \frac{1}{2}\left|\frac{\partial\psi}{\partial x}\right|^2 - \frac{g}{2}|\psi|^4 - V(x)|\psi|^2. \tag{2.4}$$

Inserting the ansatz (2.3) into equation (2.4), we find an effective Lagrangian [38] by integrating the Lagrangian density over the whole coordinate space, $\mathcal{L} = \int_{-\infty}^{+\infty} L\mathrm{d}x$. The Euler–Lagrange minimization is performed over $\mathcal{L}$ and with respect to the free parameters and the conditions $\delta\mathcal{L}/\delta\xi = 0$ where $\xi = a, b, c$ or x_c. Four coupled equations result for $(\dot{a}, \dot{b}, \dot{x}_c, \dot{c})$, are given by

$$\dot{a} = 2ab, \tag{2.5}$$

$$\dot{b} = \frac{1}{2a^4} - \frac{1}{2}[1 - 4\kappa(x_0 - x_c) + 18\lambda(x_0 - x_c)^2] - 2b^2 + \frac{gN}{2\sqrt{2\pi}a^3}, \tag{2.6}$$

$$\dot{c} = (1 + 18\lambda a^2)(x_0 - x_c) - 2\kappa(x_0 - x_c)^2 + 12\lambda(x_0 - x_c)^3 - \kappa a^2 \tag{2.7}$$

and

$$\dot{x_c} = c, \tag{2.8}$$

which can be condensed into two second-order coupled equations for the width a and the wavepacket centre x_c,

$$\ddot{a} = \frac{1}{a^3} - a[1 - 4\kappa q + 18\lambda q^2] + \frac{gN}{\sqrt{2\pi}a^2} - 9\lambda a^3 \tag{2.9}$$

and

$$\ddot{x}_c = (1 + 18\lambda a^2)q - 2\kappa q^2 + 12\lambda q^3 - \kappa a^2, \tag{2.10}$$

where $q = x_0 - x_c$ is the displacement between the centre of the harmonic term and the wavepacket. In equation (2.9), the centre of mass motion x_c is strongly coupled with the width a of the wave function through the anharmonic terms of the confining potential. When we consider an adiabatic transport such as $q = 0$, one can see that the cubic anharmonicity κ is strongly coupled with the width a in equation (2.10). Alternatively, the quartic anharmonicity λ will create

breathing mode due to the strong coupling with the width a in the case of $q = 0$. The nonlinearities introduced by atom–atom interactions do not generate any coupling with anharmonicities, as is known for harmonic traps [16].

This system generalizes the structure found for harmonic traps via invariant-based inverse engineering [16]. In the absence of anharmonicities ($\kappa = 0$ and $\lambda = 0$), the two coupled equations (2.9) and (2.10) reduce to an Ermakov equation [40] and a Newton equation [16] for a single atom (or ion) or a BEC. By contrast, equation (2.10) for the trajectory of the centre of mass x_c can be generically recovered from the Ehrenfest theorem, and is therefore immune to the precise shape of the ansatz. In what follows, we shall exploit these coupled equations to inverse engineer shortcut to adiabatic transport of BECs.

3. Inverse engineering

In this section, we focus on the fast and high fidelity transport of a BEC from a stationary state at initial position $x_0(0) = 0$ to a target state with $x_0(t_f) = d$ in a finite time t_f. The desired distance of potential is d. We will consider the cases of cubic (see §3a) and quartic (see §3b) anharmonicities individually. In particular, the trajectory $x_0(t)$ of the potential centre can be designed by using inverse engineering methods applied to the set of equations (2.9) and (2.10). Furthermore, we will provide numerical examples that confirm the effectiveness of the method.

(a) Cubic anharmonicity

Let us consider a potential with cubic anharmonicity [18],

$$V(x,t) = \frac{1}{2}(x - x_0)^2 + \frac{1}{3!}\kappa(x - x_0)^3. \tag{3.1}$$

When $\kappa \neq 0$ and $\lambda = 0$, we substitute the condition $\ddot{x}_c = \ddot{x}_0 - \ddot{q}$ into the coupled differential equations (2.9) and (2.10), which can be simplified into

$$\ddot{a} = \frac{1}{a^3} - a + \frac{gN}{\sqrt{2\pi}a^2} + 4\kappa a q \tag{3.2}$$

and

$$\ddot{q} = \ddot{x}_0 - q + \kappa a^2 + 2\kappa q^2. \tag{3.3}$$

The second equation may be regarded as a second-order differential equation for q. We require that both initial and final states are stationary states. First, we can calculate the initial and final conditions for the function q which are $q(0) = q(t_f) = Q$. By imposing $\ddot{x}_0 - \ddot{q} = 0$ in equation (3.3), one obtains

$$Q = \frac{1 - \sqrt{1 - 8a_0^2\kappa^2}}{4\kappa}, \tag{3.4}$$

where a_0 denotes the initial and final widths, which are equal. Note that the difference Q is caused by the asymmetricity of the cubic anharmonic potential. Substituting equation (3.4) into equation (3.2), we can obtain the initial width a_0 as well as the final width by imposing $\ddot{a} = 0$,

$$\frac{1}{a_0^3} - a_0 + \frac{gN}{\sqrt{2\pi}a_0^2} + 2\kappa a_0 Q = 0. \tag{3.5}$$

The value of a_0 is numerically obtained by solving equation (3.5), which is dependent on the values of the nonlinearity g and anharmonicity strength κ. The width a_0 increases when the system has either repulsive interaction or cubic anharmonicity.

Now we use inverse engineering according to the following steps. We may recall that the initial and final states are stationary states with width a_0 without excitations at the final time. Then we

royalsocietypublishing.org/journal/rsta Phil. Trans. R. Soc. A 380: 20210280

can set up the boundary conditions for width a according to equation (3.2)

$$a(0) = a_0, \quad a(t_f) = a_0 \tag{3.6}$$

and

$$\ddot{a}(0) = 0, \quad \ddot{a}(t_f) = 0. \tag{3.7}$$

Since that the chirp and velocity terms satisfy $b(0) = b(t_f) = 0$ and $c(0) = c(t_f) = 0$ in equations (2.5) and (2.8), respectively, one can find the conditions from equations (2.6) and (2.7) that

$$\dot{a}(0) = 0, \quad \dot{a}(t_f) = 0 \tag{3.8}$$

and

$$\dot{q}(0) = 0, \quad \dot{q}(t_f) = 0, \tag{3.9}$$

In addition, the boundary conditions for x_0 in equation (3.3) are imposed by

$$x_0(t_f) = d, \quad \dot{x}_0(t_f) = 0. \tag{3.10}$$

Then we set a ninth-order polynomial for $a(t) = \sum_{n=0}^{9} a_n t^n$ and fix the parameters by satisfying all the boundary conditions of equations (3.6)–(3.10). An example of the designed function a is shown in figure 2*a*. Once we obtain the function a, one can easily get the function q in equation (3.2). Finally, x_0 and x_c can be expressed easily in terms of the width a and q which is shown in figure 2*b*. Note that we fix values of g, κ and final time t_f in the example. Figure 2*a* shows the wavepacket undergoes a slight breathing and finally returns to the initial width during the non-adiabatic process. This breathing phenomena is due to the coupling term between anharmonicity κ and width a in equation (3.2): with $\kappa = 0$, the solution of equation (3.2) will be a constant width a. Figure 2*b* illustrates that the trap trajectory oscillates from the initial position and then returns to the desired position at $x_0 = d$. The corresponding time-evolution $|\psi_{\mathrm{STA}}(x,t)|^2$ is shown in figure 2*c*.

To check the performance of the STA trajectories, we define the fidelity at the final time t_f as

$$F = |\langle \psi_{\mathrm{STA}}(t_f) | \Phi_f \rangle|^2, \tag{3.11}$$

where $\psi_{\mathrm{STA}}(t_f)$ is obtained from the direct numerical simulation (split-operator method) of equation (2.1) using the STA trajectory of $x_0(t)$. The desired ground state Φ is obtained by the imaginary time-evolution technique. $\Phi_{0,f}$ denotes the initial and final ground states, respectively. Noting that we take the ground state Φ_0 as an initial state when we do the time-evolution to get the final state $\psi_{\mathrm{STA}}(t_f)$. The fidelity of the example in figure 2*c* at the final time is $F > 0.999$. The high performance of fidelity in short time with both attractive and repulsive interactions is plotted in figure 3. The oscillations are due to the fact that the Gaussian ansatz (2.3) is not the solution of BECs with atomic interactions. It is reported that fidelity is improved by using a soliton ansatz in the attractive nonlinear system [17]. Thus in this case, the strong attractive interaction will lead to the period oscillations (see dotted-green line $g = -2$) due to the Gaussian ansatz we applied in variational approach. For the case of repulsive interaction, the period is greater than the attractive one.

(b) Quartic anharmonicity

In this section, we shall concentrate on the fast transport of BEC in quartic anharmonicity. The potential reads

$$V(x) = \frac{1}{2}(x - x_0)^2 + \frac{1}{4!}\lambda(x - x_0)^4. \tag{3.12}$$

Since $\lambda \neq 0$ and $\kappa = 0$, the coupled Ermakov-like and Newton-like equations (2.9) become

$$\ddot{a} = \frac{1}{a^3} - a(1 + 18\lambda q^2) + \frac{gN}{\sqrt{2\pi}a^2} - 9\lambda a^3 \tag{3.13}$$

and

$$\ddot{q} = \ddot{x}_0 - (1 + 18\lambda a^2)q - 12\lambda q^3. \tag{3.14}$$

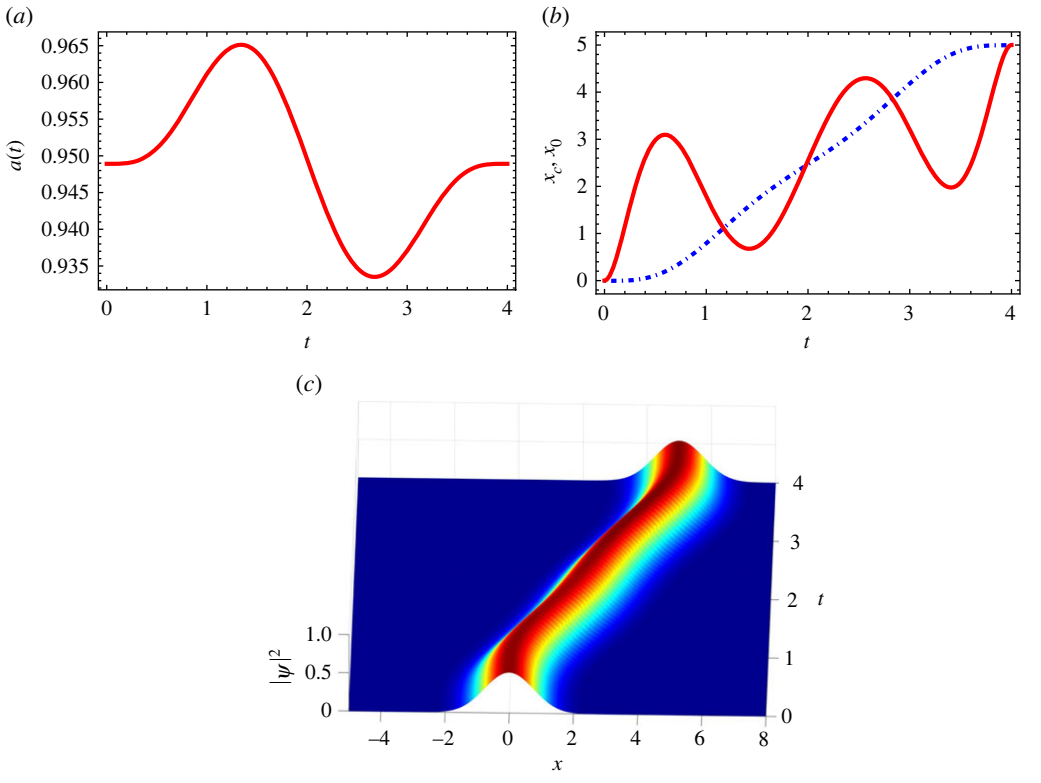

Figure 2. Cubic anharmonicity. (*a*) Width $a(t)$ with respect to time. (*b*) Designed trajectories for trap centre x_0 (red solid) and centre of mass x_c (dot-dashed blue). The rest of parameters are $Q = 4.5 \times 10^{-3}$, $a_0 = 0.95$, $g = 0.5$, $\kappa = 0.02$, $t_f = 4$, and the distance $d = 5$ of transport. (*c*) The corresponding time evolution $|\psi_{\mathrm{STA}}(x,t)|^2$. (Online version in colour.)

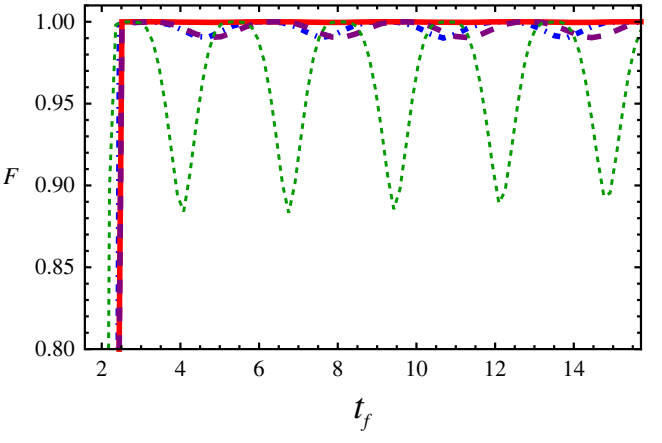

Figure 3. Cubic anharmonicity: fidelity with respect to the final time t_f for attractive atomic interactions $g = -0.1$ (red solid), $g = -0.5$ (dash-dotted blue), $g = -2$ (dotted green), repulsive interaction $g = 0.5$ (dashed purple), the anharmonic strength $\kappa = 0.02$. (Online version in colour.)

The first equation (3.13) predicts the breathing mode and the oscillations in the width of the wave packet during the transport.

Our inversion strategy will be different from the one followed previously for cubic anharmonicity because the displacement q appears quadratically in equation (3.13). We shall

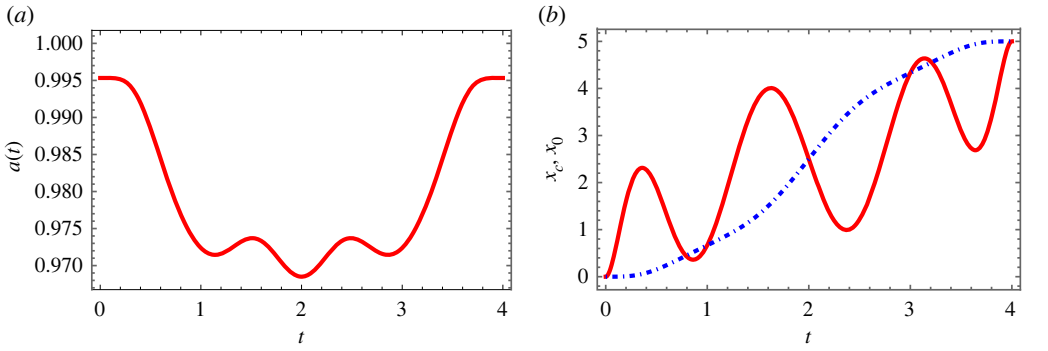

Figure 4. Quartic anharmonicity. (*a*) The width a with respect to time. (*b*) Shortcut for the designed trajectory for centre of mass x_c (dash-dotted blue) and trap centre x_0 (red solid). Parameters: $a_0 = 0.995329$, $g = 0.01$, $\lambda = 0.06$, $t_f = 4$ and $d = 5$. (Online version in colour.)

design $q(t)$ with a polynomial as $q(t) = \sum_{n=0}^{M} q_n t^n$. The boundary conditions for function q in equation (3.14)

$$\left.\begin{aligned} q(0) &= 0, \quad q(t_f) = 0 \\ \text{and} \qquad \dot{q}(0) &= 0, \quad \dot{q}(t_f) = 0. \end{aligned}\right\} \tag{3.15}$$

Then we insert the polynomial function q into the coupled equations (3.13) and (3.14) to parametrically solve the functions of width a and x_c with the conditions $a(0) = a_0$, $\dot{a}(0) = 0$ and $x_c(0) = 0$, $\dot{x}_c(0) = 0$. However, we need additional boundary conditions to achieve the final state at final time t_f, with

$$\left.\begin{aligned} a(t_f) &= a_0, \quad \dot{a}(t_f) = 0 \\ \text{and} \qquad x_0(t_f) &= d, \quad \dot{x_0}(t_f) = 0, \end{aligned}\right\} \tag{3.16}$$

where a_0 is the initial and final width calculated by equation (3.13) by imposing $\ddot{a} = 0$. The number of the boundary conditions above is eight, therefore one can choose $M = 7$. However, we want to demand the following conditions,

$$q\left(\frac{t_f}{4}\right) = 0 \quad \text{and} \quad q\left(\frac{3t_f}{4}\right) = 0, \tag{3.17}$$

to make the distance difference q between the centre of potential and the centre of wavepacket coincide at these two times. Alternative boundary conditions would be also possible. According to the above boundary conditions (3.15)–(3.17), we obtain the functions q, a, x_c and x_0. An example of the resulting trap trajectory and dynamics is shown in figure 4. Note that this stationary value makes it different from the transport of cold atoms in purely harmonic traps, since the nonlinearity and anharmonic term are involved. On the other hand, we shall also emphasize that the width a oscillates (figure 4*a*) during the transport, calculated from equation (3.13): this oscillation is again due to the coupling term between quartic anharmonicity λ and width a in the sense that with $\lambda = 0$, the solution of equation (3.13) will be again a constant width a. We are now in a position to design the shortcuts to adiabatic transport protocol. Figure 4*b* shows the trajectories of the centre of mass of wave packet and trap centre, by using inverse engineering and boundary conditions, mentioned before. At the initial and final times, the trajectories coincide with each other, which means there is no displacement deviation, guaranteeing the high fidelity ($F = 0.9999$) of the transport.

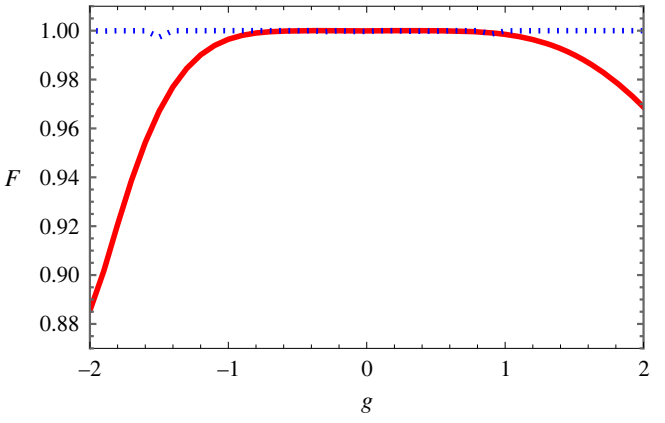

Figure 5. Fidelity for quartic $\lambda = 0.06$ (blue-dotted line), and cubic $\kappa = 0.02$ (red line) with respect to g. Other parameters are $t_f = 3\pi$, $N = 1$ and $d = 5$. (Online version in colour.)

4. Effect of nonlinearity

In this section, we shall check the fidelity of our results by solving the GPE numerically (without approximation) with the designed shortcuts. Figure 5 demonstrates that the fast transport of BECs is perfect with various anharmonic traps taking into account the attractive and repulsive interactions. The Gaussian ansatz is also valid for the variational approximation in our model in the presence of an atomic interaction $g \neq 0$. In figure 5, the fidelity for cubic anharmonicity $\kappa = 0.02$ is plotted for different atomic interactions g. The fidelity is above 0.99 for atomic interaction $|g| < 1.2$, i.e. fast transport of BEC in cubic anharmonic traps can be achieved for both attractive and repulsive interactions. The fidelity drops with interactions $|g| \geq 1.2$. This is not surprising as one would expect that the Gaussian variational approach (2.3) works better for small interaction g. For example, the nonlinearity $g = 2$ is in the range where we would not expect the ansatz to work. For $g = -2$, the fidelity will oscillate with respect to the final time which is shown in figure 3. In figure 5, the fidelity for quartic anharmonicity $\lambda = 0.06$ is plotted for different atomic interactions g. The fidelity is always greater than 0.99, i.e. fast transport of BEC in quartic anharmonic traps can be achieved for both attractive and repulsive interactions.

5. Conclusion

In summary, we present an efficient way to design high-fidelity and fast transport of BEC in anharmonic traps by combining the variational approach and inverse engineering methods. The shortcuts to adiabatic transport of the BEC are demonstrated with numerical examples in quartic and cubic anharmonicity traps. It is concluded that perfect transport can be achieved in cubic anharmonic traps in the presence of both attractive and repulsive interactions. Our method presented here is different from the previous ones [18], in which the anharmonic potential is considered as a perturbation. The shortcut trajectory can be further optimized by using optimal control theory, for instance, by taking into account noise and error in traps position and frequency [41]. The technique may be extended to three-dimensional Gaussian-beam optical traps [42], the spin-orbit coupled BECs [43], strongly interacting bosons (Tonks–Girardeau gas) [44] and superfluid Fermi gas [45]. The transport of soliton matter waves will also be reported in future work. We expect our shortcut design for fast transport to have potential applications not only in atom interferometry [46] but also in quantum information processing.

Data accessibility. This article has no additional data.

Authors' contributions. J.L.: methodology, resources, software, writing—original draft, writing—review and editing; X.C.: conceptualization, supervision, writing—review and editing; A.R.: supervision, writing—review and editing.

All authors gave final approval for publication and agreed to be held accountable for the work performed therein.

Conflict of interest declaration. We declare we have no competing interests.

Funding. J.L. and A.R. acknowledge that this publication has emanated from research supported in part by a grant from Science Foundation Ireland under grant number 19/FFP/6951 ("Shortcut-Enhanced Quantum Thermodynamics"). This work has been financially supported by EU FET Open Grant EPIQUS (899368), QUANTEK project (KK-2021/00070), the Basque Government through grant no. IT1470-22, and the project grant PID2021-126273NB-I00 funded by MCIN/AEI/10.13039/501100011033 and by "ERDF A way of making Europe" and "ERDF Invest in your Future". X.C. acknowledges the Ramón y Cajal program (RYC-2017-22482).

Acknowledgements. We are grateful to D. Rea, C. Whitty and M. Odelli for commenting on the manuscript. J.L. appreciated the discussions from J. G. Muga and D. Guéry-Odelin at early stage of work.

References

1. Milburn G. 1996 *Quantum technology*. Crows Nest, Australia: Frontiers of science. Allen & Unwin.
2. Hänsel W, Hommelhoff P, Hänsch TW, Reichel J. 2001 Bose–Einstein condensation on a microelectronic chip. *Nature* **413**, 498–501. (doi:10.1038/35097032)
3. Greiner M, Bloch I, Hänsch TW, Esslinger T. 2001 Magnetic transport of trapped cold atoms over a large distance. *Phys. Rev. A* **63**, 031401. (doi:10.1103/PhysRevA.63.031401)
4. Gustavson TL, Chikkatur AP, Leanhardt AE, Görlitz A, Gupta S, Pritchard DE, Ketterle W. 2001 Transport of Bose-Einstein condensates with optical tweezers. *Phys. Rev. Lett.* **88**, 020401. (doi:10.1103/PhysRevLett.88.020401)
5. Meschede D, Rauschenbeutel A. 2006 Manipulating single atoms. *Adv. Atomic, Mol., Opt. Phys.* **53**, 75–104. (doi:10.1016/S1049-250X(06)53003-4)
6. Lahaye T, Reinaudi G, Wang Z, Couvert A, Guéry-Odelin D. 2006 Transport of atom packets in a train of Ioffe-Pritchard traps. *Phys. Rev. A* **74**, 033622. (doi:10.1103/PhysRevA.74.033622)
7. Couvert A, Kawalec T, Reinaudi G, Guéry-Odelin D. 2008 Optimal transport of ultracold atoms in the non-adiabatic regime. *EPL (Europhysics Letters)* **83**, 13001. (doi:10.1209/0295-5075/83/13001)
8. Murphy M, Jiang L, Khaneja N, Calarco T. 2009 High-fidelity fast quantum transport with imperfect controls. *Phys. Rev. A* **79**, 020301. (doi:10.1103/PhysRevA.79.020301)
9. Lau HK, James DFV. 2011 Decoherence and dephasing errors caused by the dc Stark effect in rapid ion transport. *Phys. Rev. A* **83**, 062330. (doi:10.1103/PhysRevA.83.062330)
10. Bowler R, Gaebler J, Lin Y, Tan TR, Hanneke D, Jost JD, Home JP, Leibfried D, Wineland DJ. 2012 Coherent diabatic ion transport and separation in a multizone trap array. *Phys. Rev. Lett.* **109**, 080502. (doi:10.1103/PhysRevLett.109.080502)
11. Walther A, Ziesel F, Ruster T, Dawkins ST, Ott K, Hettrich M, Singer K, Schmidt-Kaler F, Poschinger U. 2012 Controlling fast transport of cold trapped ions. *Phys. Rev. Lett.* **109**, 080501. (doi:10.1103/PhysRevLett.109.080501)
12. Léonard J, Lee M, Morales A, Karg TM, Esslinger T, Donner T. 2014 Optical transport and manipulation of an ultracold atomic cloud using focus-tunable lenses. *New J. Phys.* **16**, 093028. (doi:10.1088/1367-2630/16/9/093028)
13. Torrontegui E, Ibáñez S, Martínez-Garaot S, Modugno M, Guéry-Odelin D, Ruschhaupt A, Chen X, Muga JG. 2013 Chapter 2 - Shortcuts to Adiabaticity. In *Advances in Atomic, Molecular, and Optical Physics* (eds E Arimondo, PR Berman, CC Lin), Advances In Atomic, Molecular, and Optical Physics, vol. 62, pp. 117–169. New York, NY: Academic Press.
14. Guéry-Odelin D, Ruschhaupt A, Kiely A, Torrontegui E, Martínez-Garaot S, Muga JG. 2019 Shortcuts to adiabaticity: concepts, methods, and applications. *Rev. Mod. Phys.* **91**, 045001. (doi:10.1103/RevModPhys.91.045001)
15. Torrontegui E, Chen X, Modugno M, Schmidt S, Ruschhaupt A, Muga JG. 2012 Fast transport of Bose-Einstein condensates. *New J. Phys.* **14**, 013031. (doi:10.1088/1367-2630/14/1/013031)
16. Torrontegui E, Ibáñez S, Chen X, Ruschhaupt A, Guéry-Odelin D, Muga JG. 2011 Fast atomic transport without vibrational heating. *Phys. Rev. A* **83**, 013415. (doi:10.1103/PhysRevA.83.013415)
17. Li J, Zhang Q, Chen X. 2017 Trigonometric protocols for shortcuts to adiabatic transport of cold atoms in anharmonic traps. *Phys. Lett. A* **381**, 3272–3275. (doi:10.1016/j.physleta.2017.08.027)

18. Zhang Q, Chen X, Guéry-Odelin D. 2015 Fast and optimal transport of atoms with nonharmonic traps. *Phys. Rev. A* **92**, 043410. (doi:10.1103/PhysRevA.92.043410)
19. Chen X, Torrontegui E, Stefanatos D, Li JS, Muga JG. 2011 Optimal trajectories for efficient atomic transport without final excitation. *Phys. Rev. A* **84**, 043415. (doi:10.1103/PhysRevA.84.043415)
20. Whitty C, Kiely A, Ruschhaupt A. 2020 Quantum control via enhanced shortcuts to adiabaticity. *Phys. Rev. Res.* **2**, 023360. (doi:10.1103/PhysRevResearch.2.023360)
21. Whitty C, Kiely A, Ruschhaupt A. 2022 Robustness of enhanced shortcuts to adiabaticity in lattice transport. *Phys. Rev. A* **105**, 013311. (doi:10.1103/PhysRevA.105.013311)
22. Whitty C, Kiely A, Ruschhaupt A. 2022 Improved anharmonic trap expansion through enhanced shortcuts to adiabaticity. *J. Phys. B: At. Mol. Opt. Phys.* **55**, 194003. (doi:10.1088/1361-6455/ac8bb7)
23. Fürst HA, Goerz MH, Poschinger UG, Murphy M, Montangero S, Calarco T, Schmidt-Kaler F, Singer K, Koch CP. 2014 Controlling the transport of an ion: classical and quantum mechanical solutions. *New J. Phys.* **16**, 075007. (doi:10.1088/1367-2630/16/7/075007)
24. Masuda S, Nakamura K. 2010 Fast-forward of adiabatic dynamics in quantum mechanics. *Proc. R. Soc. A* **466**, 1135–1154. (doi:10.1098/rspa.2009.0446)
25. Masuda S. 2012 Acceleration of adiabatic transport of interacting particles and rapid manipulations of a dilute Bose gas in the ground state. *Phys. Rev. A* **86**, 063624. (doi:10.1103/PhysRevA.86.063624)
26. Deffner S, Jarzynski C. 2014 Classical and quantum shortcuts to adiabaticity for scale-invariant driving. *Phys. Rev. X* **4**, 021013. (doi:10.1103/PhysRevX.4.021013)
27. An S, Lv D, Kim K. 2016 Shortcuts to adiabaticity by counterdiabatic driving for trapped-ion displacement in phase space. *Nat. Commun.* **7**, 12999. (doi:10.1038/ncomms12999)
28. Hänsel W, Reichel J, Hommelhoff P, Hänsch TW. 2001 Magnetic conveyor belt for transporting and merging trapped atom clouds. *Phys. Rev. Lett.* **86**, 608–611. (doi:10.1103/PhysRevLett.86.608)
29. Corgier R, Amri S, Herr W, Ahlers H, Rudolph J, Guéry-Odelin D, Rasel EM, Charron E, Gaaloul N. 2018 Fast manipulation of Bose–Einstein condensates with an atom chip. *New J. Phys.* **20**, 055002. (doi:10.1088/1367-2630/aabdfc)
30. Lobser DS, Barentine AES, Cornell EA, Lewandowski HJ. 2015 Observation of a persistent non-equilibrium state in cold atoms. *Nat. Phys.* **11**, 1009–1012. (doi:10.1038/nphys3491)
31. Bulatov A, Vugmeister BE, Rabitz H. 1999 Nonadiabatic control of Bose-Einstein condensation in optical traps. *Phys. Rev. A* **60**, 4875–4881. (doi:10.1103/PhysRevA.60.4875)
32. Li GQ, Fu LB, Xue JK, Chen XZ, Liu J. 2006 Collective excitations of a Bose-Einstein condensate in an anharmonic trap. *Phys. Rev. A* **74**, 055601. (doi:10.1103/PhysRevA.74.055601)
33. Moulieras S, Monastra AG, Saraceno M, Leboeuf P. 2012 Wave-packet dynamics in nonlinear Schrödinger equations. *Phys. Rev. A* **85**, 013841. (doi:10.1103/PhysRevA.85.013841)
34. Lu XJ, Chen X, Alonso J, Muga JG. 2014 Fast transitionless expansions of Gaussian anharmonic traps for cold atoms: Bang-singular-bang control. *Phys. Rev. A* **89**, 023627. (doi:10.1103/PhysRevA.89.023627)
35. Palmero M, Torrontegui E, Guéry-Odelin D, Muga JG. 2013 Fast transport of two ions in an anharmonic trap. *Phys. Rev. A* **88**, 053423. (doi:10.1103/PhysRevA.88.053423)
36. Kamchatnov AM, Shchesnovich VS. 2004 Dynamics of Bose-Einstein condensates in cigar-shaped traps. *Phys. Rev. A* **70**, 023604. (doi:10.1103/PhysRevA.70.023604)
37. Cohen-Tannoudji C, Guéry-Odelin D. 2011 *Advances in atomic physics*. Singapore: World Scientific.
38. Pérez-García VM, Michinel H, Cirac JI, Lewenstein M, Zoller P. 1996 Low energy excitations of a Bose-Einstein condensate: a time-dependent variational analysis. *Phys. Rev. Lett.* **77**, 5320–5323. (doi:10.1103/PhysRevLett.77.5320)
39. Impens F, Guéry-Odelin D. 2010 Classical phase-space approach for coherent matter waves. *Phys. Rev. A* **81**, 065602. (doi:10.1103/PhysRevA.81.065602)
40. Chen X, Ruschhaupt A, Schmidt S, Guéry-Odelin D, Muga JG. 2010 Fast optimal frictionless atom cooling in harmonic traps: shortcut to adiabaticity. *Phys. Rev. Lett.* **104**, 063002. (doi:10.1103/PhysRevLett.104.063002)
41. Lu XJ, Ruschhaupt A, Muga JG. 2018 Fast shuttling of a particle under weak spring-constant noise of the moving trap. *Phys. Rev. A* **97**, 053402. (doi:10.1103/PhysRevA.97.053402)

42. Torrontegui E, Chen X, Modugno M, Ruschhaupt A, Guéry-Odelin D, Muga JG. 2012 Fast transitionless expansion of cold atoms in optical Gaussian-beam traps. *Phys. Rev. A* **85**, 033605. (doi:10.1103/PhysRevA.85.033605)
43. Li J, Sherman EY, Ruschhaupt A. 2022 Quantum heat engine based on a spin-orbit and Zeeman-coupled Bose-Einstein condensate. *Phys. Rev. A* **106**, L030201. (doi:10.1103/PhysRevA.106.L030201)
44. Quinn E, Haque M. 2014 Modulated trapping of interacting bosons in one dimension. *Phys. Rev. A* **90**, 053609. (doi:10.1103/PhysRevA.90.053609)
45. Hou JX. 2014 Wave packet dynamics of superfluid fermi gases in an anharmonic trap. *J. Low Temp. Phys.* **177**, 305–314. (doi:10.1007/s10909-014-1215-4)
46. Dupont-Nivet M, Westbrook CI, Schwartz S. 2016 Contrast and phase-shift of a trapped atom interferometer using a thermal ensemble with internal state labelling. *New J. Phys.* **18**, 113012. (doi:10.1088/1367-2630/18/11/113012)